Spiraling elliptic solitons in nonlocal nonlinear media without anisotropy

Guo Liang, Qian Shou and Qi Guo*

Laboratory of Photonic Information Technology, South China Normal University, Guangzhou 510631,China

guoq@scnu.edu.cn

Abstract: The optical spatial solitons with ellipse-shaped spots have generally been considered to be a result of either linear or nonlinear anisotropy. In this paper, we introduce a class of spiraling elliptic solitons in the nonlocal nonlinear media without both linear and nonlinear anisotropy. The spiraling elliptic solitons carry the orbital angular momentum, which plays a key role in the formation of such solitons, and are stable for any degree of nonlocality except the local case when the response function of the material is Gaussian function. The formation of such solitons can be attributable to the effective anisotropic diffraction (linear anisotropy) resulting from the orbital angular momentum. Our variational analytical result is confirmed by direct numerical simulation of the nonlocal nonlinear Schrödinger equation.

OCIS codes: (190.0190)Nonlinear optics;(190.6135)Spatial solitons

References and links

1. E. D. Eugenieva and D. N. Christodoulides, "Elliptic incoherent solitons in saturable nonlinear media," Opt. Lett. **25,** 972–974 (2000).
2. M. Shen, Q. Wang and J. L. Shi, "Elliptic incoherent accessible solitons in strongly nonlocal media," Opt. Commun. **270,** 384–390 (2007).
3. O. Katz, T. Carmon, T. Schwartz, M. Segev and D. N. Christodoulides, "Observation of elliptic incoherent spatial solitons," Opt. Lett. **29,** 1248–1250 (2004).
4. Q. Guo and S. Chi, "Nonlinear light beam propagation in uniaxial crystals: nonlinear refractive index, self-trapping and self-focusing," J. Opt. A: Pure Appl. Opt.**2** 5–15 (2000).
5. A. Ciattoni and C. Palma, " Optical propagation in uniaxial crystals orthogonal to the optical axis: paraxial theory and beyond," J. Opt. Soc. Am. A, **20,** 2163–2171 (2003).
6. S. V. Polyakov and G. I. Stegeman, "Existence and properties of quadratic solitons in anisotropic media: Variational approach," Phys. Rev. E, **66,** 046622 (2002).
7. C. Rotschild, O. Cohen, O. Manela and M. Segev, "Solitons in Nonlinear Media with an Infinite Range of Nonlocality: First Observation of Coherent Elliptic Solitons and of Vortex-Ring Solitons," Phys. Rev. Lett **95** 213904 (2005).
8. X. J. Qin, Q. Guo, W. Hu and S. Lan, "Strongly nonlocal elliptical spatial optical soliton," Acta Phys. Sin. **55,** 1237–1243 (2006)(in Chinese).
9. P. Zhang et al., "Elliptical discrete solitons supported by enhanced photorefractive anisotropy," Opt. Express. **16,** 3865–3870 (2008).
10. B. Crosignani and P. Di Porto, "Nonlinear propagation in Kerr media of beams with unequal transverse widths," Opt. Lett. **18,** 1394–1396 (1993).
11. A. W. Snyder and D. J. Mitchell, "Mighty morphing spatial solitons and bullets," Opt. Lett. **22,** 16–18 (1997).
12. V. Tichonenko, "Observation of mighty morphing spatial solitons," Opt. Lett. **23,** 594–596 (1998).
13. A.S.Desyatnikov, D.Buccoliero, M.R.Dennis and Y.S.Kivshar, "Suppression of Collapse for Spiraling Elliptic Solitons," Phys. Rev. Lett **104** 053902 (2010).
14. G. Fibich and G. Papanicolaou, "Self-focusing in the perturbed and unperturbed nonlinear Schrödinger equation in critical dimension, " SIAM J. Appl. Math. **60,** 183 (1999).

15. O. Bang et al., "Collapse arrest and soliton stabilization in nonlocal nonlinear media," Phys. Rev. E **66,** 046619 (2002).
16. D. M. Deng and Q. Guo, "Ince-Gaussian solitons in strongly nonlocal nonlinear media," Opt. Lett. **32,** 3206–3208 (2007).
17. Q. Guo, B. Luo, S. Chi, "Optical beams in sub-strongly non-local nonlinear media: A variational solution," Opt. Commun. **259,** 336–341 (2006).
18. D. M. Deng, Q. Guo and W. Hu, "Complex-variable-functionCGaussian solitons," Opt. Lett. **34,** 43–45 (2009).
19. K. F. Riley, M. P. Hobson and S. J. Bence, *Mathematical Methods for Physics and Engineering*, (Cambridge, 2nd ed, 2002), pp. 165-170.
20. K. D. Moll, A. L. Gaeta and G. Fibich, "Self-Similar Optical Wave Collapse: Observation of the Townes Profile," Phys. Rev. Lett **90** 203902 (2003).
21. S. Chi and Q. Guo, "Vector theory of self-focusing of an optical beam in Kerr media," Opt. Lett. **20,** 1598–1600 (1995).
22. G. P. Agrawal, *Nonlinear Fiber Optics* (Academic, 3rd ed, San Diego, 2001), pp. 63-134.
23. D. Faccio, P. D. Trapani, S. Minardi and A. Bramati, "Far-field spectral characterization of conical emission and filamentation in Kerr media," J. Opt. Soc. Am. B, **22,** 862–869 (2005).

1. Introduction

The nonlinear propagation of optical beams with ellipse-shaped spots has been discussed during recent years. The self-trapping beams with ellipse-shaped spots can be obtained by introducing either linear anisotropy or nonlinear anisotropy. Elliptic incoherent solitons have been reported in saturable nonlinear media [1], in strongly nonlocal media [2] and in photorefractive screening nonlinear media [3], where linear anisotropy comes from the anisotropic coherence function. Furthermore, it was predicted [4] that there exists an elliptical self-trapping beam for the extraordinary light in uniaxial crystals due to the anisotropic diffraction (linear anisotropy) [5, 6]. On the other hand, coherent elliptic strongly nonlocal solitons were observed experimentally in lead glass [7] where nonlinear anisotropy is achieved by rectangular boundaries in the transverse, and were also simultaneously and independently predicted when the nonlinear response function of the medium was assumed to be anisotropic [8]. And elliptical discrete solitons can form in an optically induced two-dimensional photonic lattice where the nonlinear anisotropy comes of enhanced photorefractive anisotropy and nonlocality under a nonconventional bias condition [9].

Since optical solitons are the result of the exact balance between linearity and nonlinearity, the elliptic solitons can generally not exist in the media with both linear and nonlinear isotropy, and the ellipse-shaped beams always undergo significant oscillations in the propagation directiom in such media [10, 11, 12]. It was predicted very recently [13], however, that the elliptic solitons with the initial orbital angular momentum (OAM) can exist in such media, and they will rotate along the propagate distance. Such solitons are unstable in the (local) cubic nonlinear media, but they can propagate stably in the saturable nonlinear media because the saturable nonlinearity can arrest the collapse instability [14].

Apart from the saturable nonlinearity, there is another mechanism that is nonlocal nonlinearity can arrest the catastrophic collapse of the self-trapping beams [15]. So such class of spiraling elliptic solitons might also exis t in nonlocal nonlinear media, which will be confirmed theoretically in this paper.

2. The variational solution of the spiraling elliptic soliton

The propagation of optical beams in nonlocal cubic nonlinear media can be modeled by the following nonlocal nonlinear Schrödinger equation(NNLSE) [16],

$$2ik\frac{\partial A}{\partial \zeta}+\frac{\partial^2 A}{\partial \xi^2}+\frac{\partial^2 A}{\partial \eta^2}+2k^2\frac{n_2}{n_0}A\iint \bar{R}(\xi-\xi',\eta-\eta')|A(\xi',\eta')|^2\mathrm{d}\xi'\mathrm{d}\eta'=0, \tag{1}$$

where $A(\xi,\eta,\zeta)$ is a paraxial beam, $\bar{R}$ is the response function of the medium, ζ is the longitudinal coordinate, ξ and η are the transverse coordinates, $k=\omega n_0/c$ is the wavenumber in the media without nonlinearity, n_0 is the linear refractive index of the media, n_2 is the nonlinear index coefficient. Through the dimensionless transformation $x=\xi/w_0, y=\eta/w_0, z=\zeta/(kw_0^2), \psi=Akw_0(n_2/n_0)^{1/2}, R=w_0^2\bar{R}$, where w_0 is the initial width of the optical beam, Eq.(1) is expressed as in the dimensionless form

$$i\frac{\partial\psi}{\partial z}+\frac{1}{2}\left(\frac{\partial^2\psi}{\partial x^2}+\frac{\partial^2\psi}{\partial y^2}\right)+\Delta n\psi=0, \tag{2}$$

where $\Delta n=\iint R(\mathbf{r}-\mathbf{r}')|\psi(\mathbf{r}')|^2\mathrm{d}^2\mathbf{r}'$ is the nonlinear perturbation of refraction index with $\mathbf{r}=x\mathbf{e}_x+y\mathbf{e}_y$. $R(r)=1/(2\pi w_m^2)\exp[-r^2/2w_m^2]$ is assumed in this paper, where w_m is the characteristic length of the response function in the dimensionless system.

The Lagrangian of Eq.(2) can be expressed as [17] $L=1/2\iint(\psi^*\partial\psi/\partial z-\psi\partial\psi^*/\partial z)\mathrm{d}x\mathrm{d}y-H$, where H is the Hamiltonian of this system, $H=1/2\iint(|\partial\psi/\partial x|^2+|\partial\psi/\partial y|^2-\Delta n|\psi|^2)\mathrm{d}x\mathrm{d}y$. We introduce a trial function [13],

$$\psi(x,y,z)=\sqrt{\frac{P}{\pi b(z)c(z)}}G\left[\frac{X}{b(z)}\right]G\left[\frac{Y}{c(z)}\right]\exp(i\phi), \tag{3}$$

where the Gaussian envelope is $G(t)=\exp(-t^2/2)$, the phase is $\phi=B(z)X^2+\Theta(z)XY+Q(z)Y^2+\varphi(z)$, $X=x\cos\beta(z)+y\sin\beta(z), Y=-x\sin\beta(z)+y\cos\beta(z)$ and P is the power, $P=\iint|\psi|^2\mathrm{d}x\mathrm{d}y$. We can obtain the orbital angular momentum(OAM), $M=\mathrm{Im}\iint\psi^*(\mathbf{r}\times\nabla\psi)\mathrm{d}^2\mathbf{r}=1/2P(b^2-c^2)\Theta$. Inserting the Gaussian ansatz (3) into the Lagrangian, L can be analytically determined. Then using the variational approach, we can obtain that $P'=0, H'=0, M'=0, b'=2bB, c'=2cQ, \beta'=(b^2+c^2)\Theta/(b^2-c^2)$ and

$$\varphi'=-\frac{b^2+c^2}{2b^2c^2}+\frac{P[6b^2c^2+5w_m^2(b^2+c^2)+4w_m^4]}{8\pi[(b^2+w_m^2)(c^2+w_m^2)]^{3/2}}, \tag{4}$$

where the primes indicate derivatives with respect to the variable z. So it can be found that the power, the Hamiltonian and the OAM of the system are conservative. We can determine the Hamiltonian of the system, $H=P/4(b'^2+c'^2+\Pi)$, where

$$\Pi=\frac{1}{b^2}+\frac{1}{c^2}+\frac{4b^2\sigma^2}{(b^2-c^2)^2}+\frac{4c^2\sigma^2}{(b^2-c^2)^2}-\frac{P}{\pi\sqrt{(b^2+w_m^2)(c^2+w_m^2)}}, \tag{5}$$

with $\sigma\equiv M/P=1/2(b^2-c^2)\Theta$.

Solitons can be found as the extrema of the potential $\Pi(b,c)$. Assuming $b>c$ without loss of generality and letting $\partial\Pi/\partial b=0$ and $\partial\Pi/\partial c=0$, we can obtain the critical power and the critical OAM

$$P_c=\frac{2\pi\left(1+\rho^2\right)^3\left[\left(1+\delta^2\right)\left(1+\delta^2\rho^2\right)\right]^{3/2}}{\rho\left[1+\left(6+4\delta^2\right)\rho^2+\left(1+4\delta^2\right)\rho^4\right]}, \sigma_c=\frac{\left(\rho^2-1\right)^2\left[1+\delta^2\left(1+\rho^2\right)\right]^{1/2}}{2\rho\left[1+\left(6+4\delta^2\right)\rho^2+\left(1+4\delta^2\right)\rho^4\right]^{1/2}}, \tag{6}$$

and $M_c=P_c\sigma_c$, where $\rho=b/c$ and $\delta=w_m/b$ represent the ellipticity of the elliptic beam and the degree of nonlocality, respectively. The larger is δ, the stronger is the degree of nonlocality. When $P=P_c, \sigma=\sigma_c$, the optical beam can propagate keeping its elliptic profile changeless and rotating stably. We can also obtain the rotation velocity $\Omega_c\equiv\beta'=2(b^2+c^2)\sigma_c/(b^2-c^2)^2$. When the semi-axes b and c are given, the critical power and the critical

OAM of the spiraling elliptic solitons can be determined by Eq.(6). One example is shown in Fig.1(a) with $P_c = 1.27\times10^5, \sigma_c = 0.561, \Theta_c = 2\sigma_c/(b^2-c^2) = 0.374$ and $\Omega_c = 0.623$ when $b = 2.0, c = 1.0, w_m = 15.0$. Comparing two half widths obtained from variational solution, $w_x = (b^2\cos^2\Omega_c z + c^2\sin^2\Omega_c z)^{1/2}$ and $w_y = (c^2\cos^2\Omega_c z + b^2\sin^2\Omega_c z)^{1/2}$, with those from the numerical simulation of Eq.(2) by using $\psi(x,y,0) = [P_c/(\pi bc)]^{1/2}\exp[-x^2/(2b^2) - y^2/(2c^2)]\exp(i\Theta_c xy)$ as the input beam at $z = 0$, we find an excellent agreement as shown in Fig.1(a). The formation of the spiraling elliptic soliton is due to the effective anisotropic diffraction resulting from the OAM, which will be illustrated in the fourth part of the paper, then the ellipticity ρ of the elliptic beam should increase when the critical OAM M_c increases, as shown in Fig.2(a). In addition, the OAM can strengthen effectively diffraction against self-focusing [13], so the critical power P_c should increase together with M_c when ρ increases, as shown in Fig.2(b). Besides, P_c and M_c increase when the degree of nonlocality increases, which can also be observed in Fig. 2.

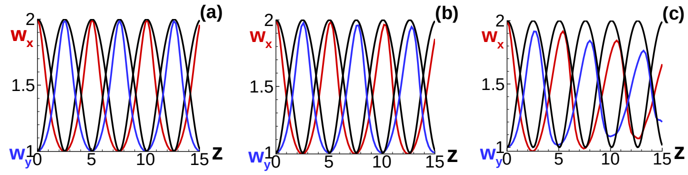

Fig. 1. (color online) Comparison of the beam width of the analytical solution (black curves) with that of the numerical simulation (red curves for w_x and blue curves for w_y) for $\delta = 7.5$ (a), $\delta = 4$ (b), and $\delta = 2$ (c).

It can be shown that the solution Eq.(3) in the strong nonlocality is equivalent to the Gaussian complex-variable-function(CVF)-Gaussian soliton, a special case of the CVF-Gaussian solitons suggested recently [18] when an arbitrary analytical function f takes the Gaussian function. For the limit of the strongly nonlocal nonlinearity, Eq.(4) and Eq.(6) can be reduced as $\varphi'|_{w_m\to\infty} = -(b^2+c^2)/(2b^2c^2), P_c|_{w_m\to\infty} = \pi w_m^4(b^2+c^2)^2/(2b^4c^4), \sigma_c|_{w_m\to\infty} = (b^2-c^2)^2/(4b^2c^2)$. If we use the variable substitutions $b^2 = \kappa^2w^2/(\kappa^2+1), c^2 = \kappa^2w^2/(\kappa^2-1)$, the spiraling elliptic soliton (3) can be deduced as $\psi(x,y,z) = \sqrt{P/(\pi bc)}\,f(\upsilon)\exp\left[-r^2/(2w^2) - i\beta\right]$, where $f(\upsilon) = \exp(-\upsilon^2/2)$ and $\upsilon = (x+iy)/(\kappa w)\exp(-i\beta)$. The expression does be the Gaussian CVF-Gaussian soliton [18], and the parameter κ here is the distribution factor b in Ref. [18].

3. Analytic stability analysis of the solution

From Eq.(6), we know that P_c and σ_c can be determined when b and c are given. It is also true in reverse. When P_c and σ_c are given first, then b and c can be obtained, which are corresponding to the stationary point of the potential function $\Pi(b,c)$. We use (b_s, c_s) to represent this stationary point here. Hence we can study the stability of our analytical soliton solution by determining whether (b_s, c_s) is the minimum point of $\Pi(b,c)$ or not. For this purpose, we expand $\Pi(b,c)$ in Taylor's series about the stationary point (b_s, c_s) to the second order [19]

$$\Pi(b,c) \approx \Pi(b_s,c_s) + \frac{1}{2}\left[\mu_1(\Delta b + \frac{\mu_2}{\mu_1}\Delta c)^2 + \frac{\mu_1\mu_3 - \mu_2^2}{\mu_1}(\Delta c)^2\right], \tag{7}$$

where $\mu_1 = \partial^2\Pi/\partial b^2\,|_{P=P_c,\sigma=\sigma_c}$, $\mu_2 = \partial^2\Pi/(\partial b\partial c)\,|_{P=P_c,\sigma=\sigma_c}$, $\mu_3 = \partial^2\Pi/\partial c^2\,|_{P=P_c,\sigma=\sigma_c}$, $\Delta b = b - b_s$ and $\Delta c = c - c_s$. We can derive that $\mu_1, \mu_3 > 0$ and $\mu_2^2 < \mu_1\mu_3$ when $w_m \neq 0$. So the stationary point (b_s, c_s) is really the minimum point of the potential function because $\Pi(b,c) - \Pi(b_s,c_s) > 0$ in this case. However, we obtain that $\mu_2^2 = \mu_1\mu_3$ when $w_m = 0$, and

Eq.(7) is deduced as $\Pi(b,c)-\Pi(b_s,c_s)\approx 1/2[\mu_1(\Delta b+\mu_2\Delta c/\mu_1)^2]$. Thus $\Pi(b,c)-\Pi(b_s,c_s)\approx 0$ along the particular direction that $\Delta b=-\mu_2\Delta c/\mu_1$, and next higher order term need to be considered in order to judge whether (b_s,c_s) is minimum point. But we can deal with the problem in a simpler way. We directly compare the value of the potential function at the stationary point (b_s,c_s) and that at the point with a displacement $(\Delta b,\Delta c)$ from the stationary point along the particular direction that $\Delta b=-\mu_2\Delta c/\mu_1$, and find that $\Pi(b_s+\Delta b,c_s+\Delta c)-\Pi(b_s,c_s)=0$. Therefore, for the case of $w_m=0$ the stationary point (b_s,c_s) is not the minimum point of the potential function yet. As a result, we can draw the conclusion that the soliton solutions are stable for any degree of nonlocality except for the local case.

It is known that the spatial profile of the optical beams in the local cubic nonlinear media will evolve to a specific circularly symmetric shape, known as the Townes profile [20] that is very different from Gaussian profile. So when the degree of nonlocality is weak enough (δ is small enough), the Gaussian trial function is not suitable any longer. The deviation between the exact solution of Eq.(2) and the trial solution Eq.(3) can bring about the disagreement of the beam width obtained from the variational approach with that from the numerical simulation, as shown in Fig.1(c) when $\delta=2$. In fact, the deviation between the variational solution and the numerical simulation was discussed in Ref. [13] for the local case. But, even so, we can find that when $\delta=4$, which is out of the region of strong nonlocality, our variational results still have a good agreement with the numerical simulations, as shown in Fig.1(b).

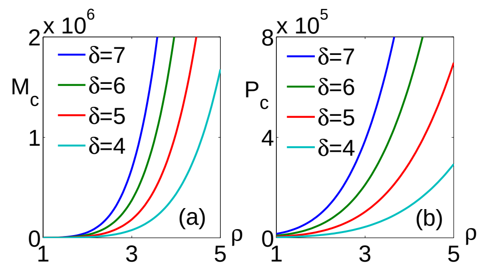

Fig. 2. (color online) Critical OAM (a) and critical power (b) as functions of the ellipticity ρ for different degree of nonlocality.

4. Physical explanation of the formation of spiraling elliptic solitons

To better understand the formation of such spiraling elliptic solitons, we turn to the analysis of the wave vector of the electric field that can be obtained by $\mathbf{k}=\nabla\overline{\phi}_{tol}$, where $\overline{\phi}_{tol}$ is the total phase of the electric field expressed as $\overline{\phi}_{tol}(\xi,\eta,\zeta)=\overline{\phi}(\xi,\eta,\zeta)+k\zeta$ in the physical coordinate system. Taking the paraxial beam into consideration, we need only take care of the wave vector $\mathbf{k}$ around some point on the propagation axis $(0,0,\zeta_0)$. We therefore can expand $\overline{\phi}(\xi,\eta,\zeta)$ with respect to (ξ,η,ζ) in Taylor's series about $(0,0,\zeta_0)$ to the second order, and obtain

$$\mathbf{k}=(\gamma_{\xi\xi}\xi+\gamma_{\xi\eta}\eta)\mathbf{e}_\xi+(\gamma_{\eta\eta}\eta+\gamma_{\xi\eta}\xi)\mathbf{e}_\eta+k\mathbf{e}_\zeta, \tag{8}$$

where $\gamma_j=\partial_j\overline{\phi}|_{\xi=0,\eta=0,\zeta=\zeta_0},\gamma_{jl}=\partial^2_{jl}\overline{\phi}|_{\xi=0,\eta=0,\zeta=\zeta_0}$ $(j,l=\xi,\eta,\zeta)$. In the equation above, we neglect the terms $\gamma_{\xi\zeta}$, $\gamma_{\eta\zeta}$, $\gamma_{\zeta\zeta}$ and γ_ζ because of the fact [21] that $\partial\overline{\phi}/\partial\zeta\ll\partial\overline{\phi}/\partial\xi$(or $\partial\overline{\phi}/\partial\eta$) for paraxial beams, and take $\gamma_\xi,\gamma_\eta=0$ (if $\gamma_\xi,\gamma_\eta\neq 0$, the wave vector would have an inclination angle with respect to the ζ-axis).

Equation (8) tells the fact that the pointing of the vector $\mathbf{k}$ at the position (ξ,η,ζ) depends upon the sign of $\gamma_{\xi\xi}$, $\gamma_{\eta\eta}$, and $\gamma_{\xi\eta}$. For simpleness, we take the projection of $\mathbf{k}$ on the $(\xi,0,\zeta)$-plane, representing by $\mathbf{k}_p$, into consideration, and the situation for the projection of $\mathbf{k}$ on the

$(0,\eta,\zeta)$-plane can be dealt with in the same way. First at the position $(\xi,0,\zeta)$, $k_\xi = \gamma_{\xi\xi}\xi$. If $\gamma_{\xi\xi} < 0$, we can reach a conclusion that $k_\xi < 0$ in the upper half plane ($\xi > 0$) and $k_\xi > 0$ in the lower half plane ($\xi < 0$). Then $\mathbf{k}_p$ points downward in the upper half plane and upward in the lower half plane, as shown in Fig.3(a). As a result, the optical beam will be contracted along the ξ direction when $\gamma_{\xi\xi} < 0$. When $\gamma_{\xi\xi} > 0$, on the contrary, $\mathbf{k}_p$ points upward in the upper half plane and downward in the lower half plane, as shown in Fig.3(b), and the optical beam will be expanded along the ξ direction. For the situation of the position $(\xi,\eta(\neq 0),\zeta)$, although the presence of the cross-talking term $\gamma_{\xi\eta}$ makes it somewhat complicated, the pointing of $\mathbf{k}_p$ can be determined in the similar way.

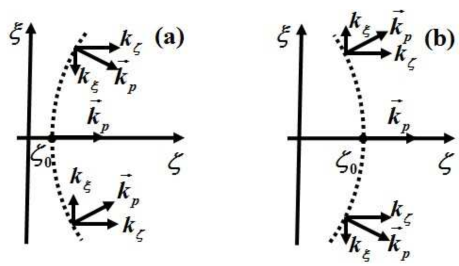

Fig. 3. Schematic of the vector $\mathbf{k}_p$ at the position $(\xi,0,\zeta)$ for $\gamma_{\xi\xi} < 0$ (a) and $\gamma_{\xi\xi} > 0$ (b). The points we consider are in fact very close to the point $(0,0,\zeta_0)$, but we have magnify the extent just for the sake of greater clarity.

The discussion above about the physical mechanism is based on the analogy of the optical beam and the optical pulse. Both of them can be dealt with in Fourier analysis—the temporal frequency of the pulse is the analogue of the spatial spectrum of the beam. Therefore, by analogy with the phenomenon of the chirp, the time dependence of the phase for the optical pulse [22], the transverse-space dependence of the phase for the optical beam can be referred to as “spatial chirp”, and the first four terms in Eq. (8) are linear spatial chirp terms (the similar concept has been introduced in Ref. [23]). As a result, the physical mechanism for the broadening (shortening) of the optical pulse [22] and the expanding (contracting) of the optical beam can be understood in this uniform sense.

On that basis, we discuss the part of the phase due to the OAM expressed as $\bar{\phi}_{OAM} = M\sin 2k\beta(-\xi^2+\eta^2)/[P(b^2-c^2)]+2\xi\eta M\cos 2k\beta/[P(b^2-c^2)]$ in the physical coordinate system, which is corresponding to $\phi_{OAM} = \Theta XY$ in the dimensionless coordinate system. Then we can obtain the part of the wave vector caused by the OAM

$$k_\xi^{(OAM)} = -\frac{2M\sin 2k\beta}{P(b^2-c^2)}\xi + \frac{2M\cos 2k\beta}{P(b^2-c^2)}\eta, k_\eta^{(OAM)} = \frac{2M\sin 2k\beta}{P(b^2-c^2)}\eta + \frac{2M\cos 2k\beta}{P(b^2-c^2)}\xi, \quad (9)$$

where $k_\xi^{(OAM)} = \partial_\xi \bar{\phi}_{OAM}, k_\eta^{(OAM)} = \partial_\eta \bar{\phi}_{OAM}$. From Eq.(9) we can find that the contributions of OAM to the wavevector are different (asymmetric) in ξ-direction and η-direction, because the signs of the two first terms in Eq. (9) are opposite. In other words, OAM can result in an effective anisotropic diffraction. It is the effective anisotropic diffraction that leads to the formation of elliptic solitons.

5. Conclusion

We have obtained spiraling elliptic solitons in nonlocal nonlinear media without anisotropy by use of the variational approach. The formation of such solitons is due to an effective anisotropic diffraction resulting from the orbital angular momentum. We show that this class of solitons are

stable for any degree of nonlocality except the local case. Our approximate analytical results have been confirmed by direct numerical simulations of the NNLSE.

Acknowledgments

This research was supported by the National Natural Science Foundation of China (Grant Nos. 11074080 and 10904041), the Specialized Research Fund for the Doctoral Program of Higher Education (Grant No. 20094407110008), and the Natural Science Foundation of Guangdong Province of China (Grant No. 10151063101000017).